Delay analysis and time-critical protocol design for in-vehicle power line communication systems

Article (Accepted Version)

Delay Analysis and Time-Critical Protocol Design for In-Vehicle Power Line Communication Systems

Zhengguo Sheng, Daxin Tian, Victor C.M. Leung and Gaurav Bansal

***Abstract*—With the emerging automated tasks in vehicle domain, the development of in-vehicle communications is increasingly important and subjected to new applications. The use of vehicular power lines has been a promising alternative to in-vehicle communications because of elimination of extra data cables. In this paper, we focus on the latest HomePlug Green PHY (HPGP) and explore its opportunity to support time-critical in-vehicle applications. Specifically, we apply Network Calculus to evaluate the worst access and queuing delay of various priority flows in vehicle bus networks. In order to maximize the bandwidth utility and satisfy the end-to-end hard delay requirements, we further propose a bandwidth efficient fair rate scheduling and delay sensitive traffic shaper. Performance evaluation supplemented by numerical and simulation results is also provided to show the advantage of HPGP and the proposed traffic shaper over the existing industry solutions.**

***Index Terms*—Vehicular power line communications, HomePlug GP, end-to-end worst delay, traffic shaper, Network Calculus.**

I. Introduction

In modern vehicles, electronics has become one of the most important components and is expected to increase exponentially with the development of advanced and connected vehicles [1]. Today's vehicles have more than 2,000 wires with the weight of 20 to 50 Kilograms. The challenge to increase the number of in-vehicle electronic systems has put considerable pressure on automotive communication networking to accommodate increasing in-vehicle information flows. Communication networks in modern vehicles use several communication buses to support control, safety and multimedia services, etc. Future applications, such as advanced driver assistance systems (ADAS), connected and autonomous vehicles, demand a highly dynamic and mission-critical in- and inter-vehicle communication environment.

In practice, a number of legacy in-vehicle communication buses, such as controller area network (CAN) [2] and local interconnect network (LIN) [3], are highly application specific and usually interconnected in heterogeneous networks via gateways. To cope with the increasing bandwidth demand of future applications, a number of recent studies use Ethernet with IEEE 802.1 audio video bridging (AVB) [4], [5] as in-vehicle network to deliver multimedia services. The on-going research of AVB towards time-sensitive networking (TSN) [6] will further extend its capability to support stringent real-time vehicle applications. However, the application of different network technologies and point-to-point links leads to an inflexible network architecture and a complex cable harness in vehicles, due to wiring complexity that affects maintenance, reliability, weight, and costs, etc.

The use of vehicular power line communications (VPLC) is promising to in-vehicle applications. So far, latest research efforts have been focused on the development of LIN, CAN and Ethernet based protocols over power line [7], [8]. Also in our recent work [9], we adopted a cross-layer approach to integrate VPLC physical layer characteristics with medium access control (MAC) and proposed a multi-channel CAN-based MAC protocol for VPLC networking. However, industry PLC solutions have been developing for more than a decade. For example, the HomePlug has different specifications to support a variety of applications, ranging from high speed HDTV to low energy smart meter application. The latest HomePlug Green PHY (HPGP) has been promoted by major automotive manufacturers as the common communication interface to facilitate the integration of electric vehicles into smart grid applications, and it will be capable to support Internet protocols into vehicles and thus enable connected vehicles. However, HomePlug, which is designed for non-critical applications in home environment, has never been considered in time-critical vehicle environment. Hence there is a lack of understanding of fundamental limits of standard HPGP in supporting in-vehicle traffic flows with various priorities and delay requirements.

In this paper, we are seeking answers to the fundamental question: whether HPGP can support critical delay requirements of in-vehicle applications and how well they can be supported? Moreover, considering that in-vehicle networks are expected to continue growing in both size and complexity, we make novel contributions to design new VPLC protocols and mechanisms for managing communications and, in particular, for ensuring end-to-end quality-of-services (QoS). By doing that, we firstly employ a deterministic modeling approach, that is Network Calculus (NC) [10], [11], to characterize the worst delay performance of real-time in-vehicle transmission using HPGP. NC has been recently developed as a powerful tool to model and analyze congestion control of switch ethernet, cellular networks, machine-to-machine and IEEE 802.11 net-

This research was sponsored by The Engineering, and Physical Sciences Research Council (EPSRC) (EP/P025862/1), Royal Society-Newton Mobility Grant (IE160920), Asa Briggs Visiting Fellowship from University of Sussex and The National Natural Science Foundation of China under Grant Nos. 61672082, U1564212 and 61711530247 (Corresponding Author: Daxin Tian).

Z. Sheng is with Department of Engineering and Design, University of Sussex, UK. E-mail: z.sheng@sussex.ac.uk.

D. Tian is with School of Transportation Science and Engineering, Beihang University, Beijing 100191, China. E-mail: dtian@buaa.edu.cn.

V. Leung is with the Department of Electrical and Computer Engineering, University of British Columbia, Canada. E-mail: vleung@ece.ubc.ca

G. Bansal is with Toyota InfoTechnology Center, USA. E-mail: gbansal@us.toyota-itc.com.

works [12]–[15]. However, there is no such a work on the analysis of contention based access protocol for in-vehicle networks. Specifically, by deriving the arrival and service processes of priority flows over a multiple access channel, hard delay bounds can be obtained, which in turn can help us understand the suitability of standard HPGP in supporting in-vehicle applications.

Providing only access control cannot ensure delay requirement from an end-to-end (E2E) point of view, particularly when a message needs to be queued and forwarded from one subsystem to another. The IEEE 802.1 AVB over switch Ethernet is being actively considered as a promising solution to automotive time-sensitive applications [4]. Given the in-vehicle flow data (i.e., priority, cycle rate, data rate and size) and static topology (e.g., tree-topology), the contention problem has been shifted to a congestion problem on switch ports. Since the AVB relies on a coordinated share network to deliver predictable performance, the challenge to incorporate AVB with HomePlug for in-vehicle applications is to ensure an access method with bounded delay, which can be solved by the NC based analytical results. Moreover, the E2E delay of time-critical in-vehicle applications are often with hard requirements, which cannot be fully satisfied by the current AVB. A new delay-sensitive traffic shaper incorporating delay deadline and priority will be devised to ensure the E2E delay requirements.

The following summarizes our contributions and key results:

- We analyze the worst delay performance of HPGP over a shared power line bus using NC tool. Such obtained results relating to priority, data rate and delay can provide useful guidelines in determining the optimal frame length and scheduling strategy for bandwidth efficient HPGP in vehicle environment.
- By further considering the data congestion on switch ports, we characterize the queuing delay for each priority flow and propose a delay sensitive credit-based traffic shaper to ensure the E2E delay requirements. A mathematical framework is also supplemented to analyze the worst delay performance of the proposed protocol under realistic data modeling.
- The analytical results show that the HPGP can achieve competitive performance compared with the existing ones, and the proposed solutions can maintain a satisfactory hard delay performance for all priority flows.

The rest of the paper is organized as follows. In section II, we review the state-of-arts and emphasize the motivation and importance of our work. In Section III, we describe the in-vehicle network topology, delay definition and data modeling of HPGP. Section IV provides the preliminary result of delay bound obtained by NC tool, whereas in Section V, we present the mathematical analysis of the worst access delay and the proposed priority-weighted fair rate scheduling. We further analyze queuing delay in Section VI and introduce the delay sensitive traffic shaper to ensure E2E delay performance. The performance evaluation is provided in Section VII, and concluding remarks are given in Section VIII.

II. Related work

Vehicular communications have been widely deployed for supporting diverse vehicle applications. Most of in-vehicle applications with time critical nature, such as brake and engine controls, are preferring dedicated wired networks for reliable and secure transmission. According to [16], the growth of automotive electronics is in the order of n^2 where n is the number of electronic control unit (ECU). This paper is motivated by the emerging VPLC technology that can support vehicle communications, especially future vehicles with highly sophisticated electronic systems, with reduced data wiring and cost.

Understanding the characteristics of power wires in vehicle as a communication channel has been the drive for many measurement campaigns [17]–[19]. The findings show that vehicle power lines constitute a harsh and noisy transmission medium with both time and frequency-selective channel, colored background noise, and periodic and aperiodic impulsive noise. The measurements in [20], [21] have confirmed that the physical transmission of PLC in vehicle is feasible. However, the emerging new challenges come with a surge in networking technology (MAC layer and above) to achieve time-critical and reliable applications, which is very limited in the existing literature.

The time critical applications can be fundamentally different from the general applications for which current MAC protocols are designed [22]. In wireless sensor networks, most existing MAC protocols are energy efficient, e.g., IEEE 802.15.4 and Wi-Fi. These protocols are typically not suitable for vehicular read-time application. Although there are advantages to use wireless transmission [23], in-vehicle wireless devices still require connections to the power source, which mitigates this advantage [24]. There are also concerns with security in wireless networks, such as eavesdropping on a in-vehicle network and reverse engineering to jam false data [25]. This particularly important, since the in-vehicle network is safety-critical and it is imperative to avoid security problems which lead to disastrous safety implications.

The existing MAC protocol design for VPLC is primarily based on the legacy in-vehicle bus protocols. LIN, which has been applied over PLC [3], [7], is a low cost serial bus network used for distributed body control electronic systems in vehicle. It is a single master/multiple slave architecture. As it is time triggered, message latency is guaranteed. However, since the speed is only 20 Kbps, it is considered to be most appropriate for less time critical applications, such as controlling doors or seats. CAN [2] is a priority-based bus which uses carrier sense multiple access with collision detection and resolution (CSMA/CDR). A more recent work [9] proposed a cross-layer approach to multiplex time and frequency variation of physical medium into CAN design for VPLC networking. However, the use of bit-wise arbitration scheme intrinsically limits the bit rate of CAN as the bit time must be long enough to cover the

propagation delay on the whole network. It supports speeds up to 1 Mbps, which is suitable for real time control applications.

The adoption of HomePlug into vehicle communications has been considered until recently [26]–[28], in which the authors proposed modified HomePlug and IEEE 1901 protocols for in-car PLC. However, it is not clear what is the fundamental limit of the solution in handling time-critical in-vehicle data transmission. Moreover, given the complexity of in-vehicle topology, its E2E worst delay analysis has never been investigated. There are existing literatures in analyzing the congestion delay using NC. The authors in [29] firstly used the NC to analyze the queuing delay of Ethernet switch networks. Later on, the similar approach has been extended to the in-vehicle network scenarios and the authors in [30], [31] analyzed the congestion delay of Ethernet and AVB based in-vehicle networks. The authors in [32] discussed the traffic shaper of AVB in vehicle networks for multimedia services. However, all of these work are Ethernet based and primarily focus on multimedia services in vehicles.

Our contribution in this paper is to analyze the worst delay performance of HPGP in vehicle environment, and further propose new designs of scheduling and traffic shaping to better utilize the bandwidth resource and guarantee a hard delay performance for mission-critical in-vehicle communications.

III. In-Vehicle Network Topology and Data Modeling

A. In-Vehicle Network Topology and Delay Definition

Fig. 1 (a) shows the hierarchical structure of in-vehicle power system, and its power line communication topology can be generalized as Fig. 1 (b). The in-vehicle networks are usually composed of a number of systems, such as infotainment and powertrain systems. Each of these systems may also include several subsystems which include a number of sensors or ECUs. We divide the whole in-vehicle networks into the following three domains:

- **Subsystem domain**: ECU is an embedded system and plays as a hub to control a subsystem in a transport vehicle. Sensor devices are directly connected to the ECU as source inputs. Hence the star-topology is primarily considered in subsystems.
- **Bus-system domain**: In order to deliver efficient communications, multiple ECUs are connected over bus-based networks and each ECU may send or receive a message with a pre-configured priority.
- **Cross-system domain**: Once a message needs to be sent across domains, a switch or gateway is needed to forward the message. The switch is configured with priority queues. Messages with the same priority need to be queued following the First-in-First-out (FIFO) rule.

In this paper, we focus on the delay incurred in the transmission process, including scheduling, transmitting and queuing. Considering the speed of switch processing is much faster than that of message queuing and transmission, we assume that when one message arrives at the switch, it will be immediately released on to a queue for forwarding with a negligible processing time [33]. Also, the propagation delay is negligible compared with other delay components. Therefore, the E2E delay is defined as

$$D_{E2E} = d_{access} + d_{trans} + d_{queue}\,. \tag{1}$$

It is noted that (1) plays as a basis for the delay analysis and can be applied to more complex network scenarios, e.g., multi-hops networks.

TABLE I
Parameters used for data modeling

Parameter	Description
N	Number of priority flow or contending node in a collision-free scenario
C_{BP}	Beacon period of HPGP
F_i	Transmission frequency of priority i
$f(i)$	Cycle rate of the priority flow i
L_s	Frame length of short MPDU
$A_i(t)$	Arrival flow of priority flow i until time t
$A_i^h(t)$	Cumulative arrival flow with priority higher than i until time t
$\alpha_i(t)$	Arrival curve of priority flow i until time t
$\alpha_i^h(t)$	Cumulative arrival curve of flow with priority higher than i until time t
σ_i	The maximum burst data size of priority flow i
ρ_i	The average rate of priority flow i
ρ_i^h	Cumulative average rate of flow with priority higher than i
R	Channel capacity
$\beta_i(t)$	Service curve of priority flow i on channel
R_i	Service rate of priority flow i on channel
T_i	Latency component of service curve i on channel
d_i	Access delay of priority flow i
$d_i^{\max}$	The maximum delay deadline of priority flow i
$L_{\max}$	The maximum frame length supported by the proposed HPGP
N_{PB}	The maximum number of physical blocks supported by HPGP
R_{IS}	Idle-slope in the credit-based traffic shaper
R_{SS}	Send-slope in the credit-based traffic shaper
$\eta = \left\lvert \frac{R_{IS}}{R_{SS}} \right\rvert$	Forwarding efficiency of SR class
t_{acc}	Time duration of accumulating credit
R^i	Service rate of priority flow i on switch
$\beta^i(t)$	Service curve of priority flow i on switch
T^i	Latency component of service curve i on switch
d^i	queuing delay of priority flow i
D_{E2E}^i	End-to-end delay of priority flow i

B. Data Modeling

Table I summarizes all parameters defined in the paper. The cycle length of HPGP (or beacon period) is defined as $C_{\text{BP}} = 40\,\text{ms}$, which is preconfigured by the central coordinator (CCo) to match a cycle frequency of 50 Hz based on the network time base. $i \in \{1, 2, ..., N\}$ denotes the priority level of flows and N corresponds to the lowest priority. The HPGP defines 4 priority levels, thus we have $N = 4$. The transmission frequency of a priority flow i can be defined as $F_i = f(i) \cdot C_{\text{BP}}$, which means that a new transmission can

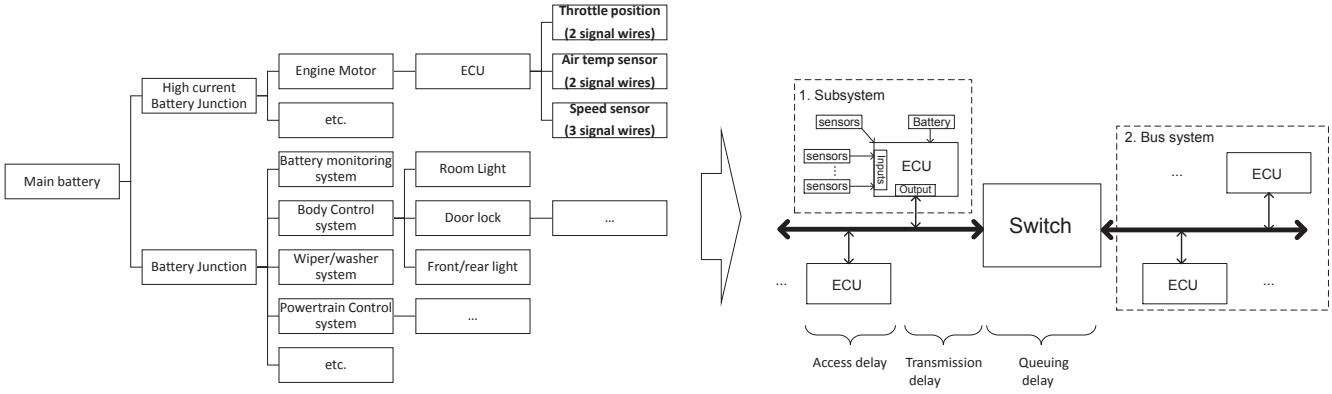

(a) Wiring diagram of a typical in-vehicle power system

(b) In-vehicle data network topology

Fig. 1. Mapping from in-vehicle power wiring harness to data network topology

be scheduled every F_i time. The $f(i)$ is the cycle rate of the priority flow i. For example, if we consider a case that a higher priority flow needs to be transmitted more frequently, we may have $f(i) = i$. Since all flows are sent in a cyclic manner, the least common multiple (lcm) of transmission frequencies of all priority flows is $F = \text{lcm}\{F_1, F_2, ..., F_N\}$. It is noted that the cycle time of real in-vehicle traffic can be varied from 10 ms up to 500 ms depending on the applications [34]. In this paper, the predefined traffic pattern of HPGP for all priority levels can be applied for control traffic class in vehicles [24], i.e., $10 - 100$ ms.

TABLE II
DATA TRAFFIC REQUIREMENTS FOR IN-VEHICLE APPLICATIONS

Traffic class	Max delay	Data rate
Control & Management	10 ms [34]	20 Kbps-1 Mbps
Safety data (audio)	33 ms [35]	64 Kbps-1.4 Mbps
Infotainment data	150 ms [36]	$\sim$ 1.5 Mbps

The general in-vehicle traffic requirement is categorized in Table II, which should be complied by existing in-vehicle communication buses. For example, the LIN bus, which is primarily used in the body and comfort domains, can support 8 byte data with low safety requirement. The CAN bus, which is used in powertrain and driver assistant control domains, can support up to 8 byte data but with stringent delay and transmission rate requirements. Therefore, given a typical in-vehicle frame length of up to 8 byte, we consider the same case [26] where the short MAC protocol Data Unit (MPDU) with only frame control (128 bits) is employed by HPGP for in-vehicle communications purposes. Fig. 2 shows the MAC schedule of HPGP. By further employing the Mini-ROBO transmission rate of 3.8 Mbps, we can have the total transmission time of such a frame as 658.08 μs, which includes 2 priority resolution slots (35.84 μs per slot), an average of 3.5 backoff slots (35.84 μs per slot), one control frame (110.48 μs), one response interfame space (RIFS) (a default

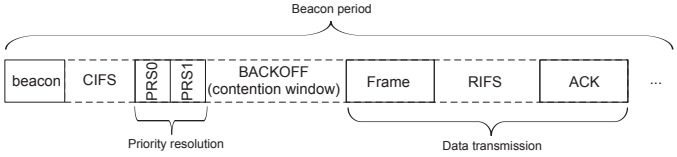

Fig. 2. HomePlug Green PHY CSMA/CA medium access

value of 140 μs[1]), one acknowledgement (110.48 μs) and one contention interframe space (CIFS) (a default value of 100 μs). Therefore, the equivalent total frame length of short MPDU can be derived as as $L_s = 2500$ bits, which includes the aforementioned protocol overhead and data frame.

IV. PRELIMINARIES: ACCESS DELAY BOUNDS OF HPGP

A. Arrival curve

The actual HPGP medium access is performed cyclic, a successful transmission depends on its own priority and contention from other flows. According to the definition in [10], the arrival flow of a message type with priority i is a cumulative function and can be derived as the step function

$$A_i(t) = \left\lceil \frac{t}{F_i} \right\rceil \cdot L_i \,, \tag{2}$$

The cumulative arrivals with priority higher than i can be derived as

$$A_i^h(t) = \sum_{i=1}^{i-1} A_i(t) = \sum_{i=1}^{i-1} \left\lceil \frac{t}{F_i} \right\rceil \cdot L_i \,, \tag{3}$$

In order to ease the analysis of the deterministic performance of networks, the upper bounded arrival curve (3) can be characterized by the well known token bucket controller concept which is defined as $\alpha_i(t) = \sigma_i + \rho_i \cdot t$, where σ is the maximum amount of flow that can arrive in a burst and ρ is the average rate of flow. Additionally, the data arrival rate is

[1]Since the HPGP is a subset of HomePlug standard, the default value can ensure the compatibility with other HomePlug standard, e.g., AV.

limited by the link capacity which is denoted as R. Thus the arrival curve can be defined as

$$\alpha_i(t) = \min\left\{R \cdot t, \sigma_i + \rho_i \cdot t\right\}, \tag{4}$$

In essence, the arrival curve for a particular priority flow can be characterized by (R, σ_i, ρ_i). In our case, the burst of each priority flow can be assumed as $\sigma_i = L_i$, which means that an immediate transmission can happen at $t = 0$. The average rate of a flow can be defined as $\rho_i = \frac{L_i}{F_i}$. Consequently, the linear expression of cumulative arrivals with priority higher than i can be obtained as

$$\alpha_i^h(t) = \min\left\{R \cdot t, \sigma_i^h + \rho_i^h \cdot t\right\}. \tag{5}$$

where $\sigma_i^h = (i-1) \cdot L_i$ and $\rho_i^h = \sum_{j=1}^{i-1} \frac{L_j}{F_j}$. We can observe that $\alpha_i^h(t) \geq A_i^h(t)$ when $t \geq 675\,\mu$s, which means the derived upper arrival curve holds for almost entire network observation and thus can satisfy all constraints of an affine arrival curve in network calculus.

B. Service curve

After we have the arrival curve for the incoming flow over a shared channel, we need to determine the service curve to reflect the communication behavior of HPGP. The outgoing flow, which is served by the communication channel, can be modeled by a family of simple service curve called the rate-latency service curve $\beta(t) = R \cdot (t - T)^+$. Consider the priority of individual flow and the non-preemptive nature of transmission mechanism, we derive the service curves for each strict priority (SP) traffic as follows.

1) Highest priority: It can always grant channel access to the highest priority traffic, unless there is a lower priority frame in transmission. Thus the rate-latency curve is

$$\beta_1(t) = R_1 \cdot (t - T_1)^+. \tag{6}$$

where $R_1 = R$ and $T_1 = \frac{max\{L_i | i \in 2...N\}}{R}$ which is the maximum transmission latency of a lower priority data. For example, if we consider to assign L_s for all priority flows, then $T_1 = 658.08\,\mu s$.

2) Middle priority: According to the SP principle, any lower priority flow needs to wait until all higher priority flows are served. So there is an additional latency for processing the initial burst imposed from higher priority flows. According to the aggregate traffic modeling of non-preemptive priority flows [29], the equivalent service rate is limited to $R - \sum_{j=1}^{i-1} \rho_j$. Thus the service curve is derived as

$$\beta_i(t) = R_i \cdot (t - T_i)^+. \tag{7}$$

where $R_i = R - \sum_{j=1}^{i-1} \rho_j$ and $T_i = \frac{\sum_{j=1}^{i-1} \sigma_j}{R_i} + T_1$. The result can be applied to characterize the second and third priority flows in HPGP.

3) Lowest priority: The only latency imposed for this flow is the waiting time to serve all higher priority flows, so we can derive the service curve for the lowest priority flow as

$$\beta_N(t) = R_N \cdot (t - T_N)^+. \tag{8}$$

where $R_N = R - \sum_{i=1}^{N-1} \rho_i$ and $T_N = \frac{\sum_{i=1}^{N-1} \sigma_i}{R_N}$. We can observe that the service curve of one flow highly depends on other flows. Particularly, with lower priority of a flow, its service curve tends to decrease.

C. Delay bound

Theorem 1: The maximum access delay bound [2] for each priority flow in HPGP is

$$d_i \leq T_i + \frac{\sigma_i \cdot (R - R_i)}{(R - \rho_i) \cdot R_i}. \tag{9}$$

Proof: According to the definition in [10], the delay bound of a flow i is the maximum horizontal deviation between its arrival curve α_i and service curve β_i. Thus we have

$$d_i \leq \sup_{t \geq 0}\{\inf\{\tau \geq 0 : \alpha_i(t) \leq \beta_i(t+\tau)\}\}$$

$$\Rightarrow d_i \leq \sup_{t \geq 0}\{\inf_{\tau \geq 0:}\{\min\left\{R \cdot t, \sigma_i + \rho_i \cdot t\right\} = R_i \cdot (t + \tau - T_i)^+\}\}, \tag{10}$$

According to min-plus algebra, the distributivity of $\sup$ and $\inf$ with respect to operators $\vee$ (max) and $\wedge$ (min) can lead (10) into

$$d_i \leq \sup_{t \geq 0}\{\inf_{\tau \geq 0:}\{R \cdot t = \beta_i(t+\tau)\} \wedge \inf_{\tau \geq 0:}\{\sigma_i + \rho_i \cdot t = \beta_i(t+\tau)\}\}, \tag{11}$$

Since we know that when $t \leq \frac{\sigma_i}{R - \rho_i}$, $R \cdot t \leq \sigma_i + \rho_i \cdot t$, we can further derive (11) as

$$\begin{aligned} d_i \leq \quad & \sup_{0 \leq t \leq t_i^*}\{\inf_{\tau \geq 0:}\{R \cdot t = R_i \cdot (t + \tau - T_i)^+\}\} \\ & \vee \sup_{t \geq t_i^*}\{\inf_{\tau \geq 0:}\{\sigma_i + \rho_i \cdot t = R_i \cdot (t + \tau - T_i)^+\}\}, \end{aligned} \tag{12}$$

where $t_i^* = \frac{\sigma_i}{R - \rho_i}$ denotes the curving point of arrival curve.

For $t \geq T_i - \tau$, (12) leads to

$$\begin{aligned} d_i \leq \quad & \sup_{0 \leq t \leq t_i^*}\{\inf_{\tau \geq 0:}\{\tau = \frac{\sum_{i=1}^{i-1} \rho_i \cdot t}{R_i} + T_i\}\} \\ & \vee \sup_{t \geq t_i^*}\{\inf_{\tau \geq 0:}\{\tau = \frac{\sigma_i + (\sum_{i=1}^{i} \rho_i - R) \cdot t}{R_i} + T_i\}\}. \end{aligned} \tag{13}$$

Due to the linear increasing and decreasing of inner equations with respect to t in (13), the result is obtained when $t = t_i^*$. □

[2]It represents the interval from the time when a frame reaches the head-of-line and ready for transmission to the beginning of the successful transmission.

D. Direct application in subsystem domain

From Section III-B, it is not difficult to observe that the original HPGP can accommodate up to 4 collision-free scheduling, i.e., 4 priorities. Although the number of supported con-current transmission is limited, it still can be applied into some of the subsystem scenarios, such as in Fig. 1 (b) in which each sensor node may have a few data wirings connected to the ECU. Table III shows an example of data wring specification of sensor nodes connected to DTA S80Pro ECU [37]. It is worth noting

TABLE III
AN EXAMPLE OF INPUT WIRING HARNESS OF S80PRO ECU

S80Pro ECU	
Inputs	No. of signal wires
Speed sensor	3
Cam position sensor	3
Air temperature sensor	2
Oil pressure sensor	1
Throttle position sensor	2

that each of these signal wires needs a dedicated data cable. For example, besides the power cable, the throttle position sensor needs additional two cables to provide throttle position and idling signals. Given most of sensor devices require no more than 4 signal cables, the original HPGP can be directly applied to schedule sensor level communications with ECU using only power wiring.

Result 1: The upper bound of maximum access delay by using HomePlug GP for in-vehicle transmission with a frame size up to 8 bytes is 2.1 ms.

Proof: The delay performance is deteriorated with a decreasing priority level. Therefore, the worst delay performance can be expected when the transmission is assigned with the lowest priority. According to (9), we can derive the maximum delay as

$$d_4 \leq T_4 + \frac{\sigma_4 \cdot (R - R_4)}{(R - \rho_4) \cdot R_4} = \frac{3 \cdot L_s}{R - \rho_i^h} + \frac{L_s \cdot \rho_i^h}{(R - \rho_i)(R - \rho_i^h)}. \tag{14}$$

where $\rho_i^h = \sum_{j=1}^{3} \frac{L_s}{F_i}$. The maximum value of d_4 can be obtained when ρ_i^h and ρ_i are the maximum, that is, when F_i is the smallest. Since $F_i = f(i) \cdot C_{\text{BP}}$, we can have all priority flows with the highest frequency of transmission $F_1 = F_2 = F_3 = F_4 = C_{\text{BP}}$, which leads to the result. □

E. Limitations of HPGP

Result 1 indicates that HPGP can satisfy the maximum delay requirement particularly for control traffic class defined in Table II, i.e., 10 ms. However, as observed from Fig. 4, the total bandwidth utility of HPGP is quite low with only about 3.4% (0.13 Mbps/3.8 Mbps). There is a significant potential to better utilize HPGP to accommodate more nodes on a sharing bus or cope with bandwidth demanding applications, such as infotainment and multimedia. Moreover, recall from Section I, the deployment of new sensors or applications in a vehicle has significantly increased the number of ECUs over a single bus system. More than 10 ECUs is quite common in today's high-speed vehicle networks. Due to the limitation of HPGP, a maximum of 4 priority flows cannot ensure collision-free transmission when more than 4 nodes are sharing the single bus.

In the following, we will propose a compatible solution of HPGP to enable more collision-free communications over a single bus, and maximize the bandwidth utility without violating delay requirements.

V. COLLISION-FREE AND BANDWIDTH EFFICIENT TRANSMISSION BASED ON HPGP

A. The Proposed Collision-Free Solution

Motivated by the CAN bus that nodes use a n-bit random arbitration register (RAR) to avoid collision and prioritize their access to the medium, the MAC mechanism of HPGP can thus be converted to support more collision-free transmission. As shown in Fig. 2, HPGP uses 2 slots for priority resolution followed up to 7 slots for backoff in a contention window. All these time slots are with identical length, i.e., 35.84 μs per slot. In practise, the backoff slots can be merged into priority resolution slots, depending on the number of nodes on a single bus. Hence the total number of priority can be significantly increased to cope with a large number of ECUs, i.e., $2^9 = 512$ ECUs. For example, if there are 10 ECUs sharing a single bus, only 2 backoff slots need to be merged with the priority resolution slots, which is capable of supporting up to $N = 2^4 = 16$ ECUs. Therefore, in the following, only priority resolution slot is considered before frame transmission. Table IV shows the updated data model when the proposed solution is applied. It is worth noting that the proposed solution does not increase the complexity of frame overhead and can coexist with standard HPGP.

TABLE IV
UPDATED DATA MODEL FOR COLLISION-FREE TRANSMISSION WHEN $N > 4$ BASED ON HPGP

N	No. of priority slots	Total transmission time of a frame (μs)	Equivalent frame length (L_s)
$4 < N <= 8$	3	568.48	2160
$8 < N <= 16$	4	604.32	2296
$16 < N <= 32$	5	640.16	2432

Result 2: Given a hard delay deadline of a mission-critical transmission $d_{\max}$, the maximum frame length that can be supported by the proposed HPGP is defined in (16).

Proof: According to (14), the lowest priority flow experiences the longest transmission delay. Therefore, in order to ensure a hard delay requirement in priority based access channel, a transmission should be considered with lowest priority in the worst scenario. Assume there are a total of N contenting nodes[3], the worst delay performance is when $F_1 = F_2 ... = F_N = C_{\text{BP}}$, thus we can obtain (15). Since the maximum total transmission rate cannot excess the channel capacity, that is, $\frac{NL_{\max}}{C_{\text{BP}}} \leq R$, the maximum frame length (16) can be obtained. □

[3]In this paper, we use N to denote both the number of priority flow and the number of contending node, since they are identical in collision-free scenarios.

$$
\begin{aligned}
&d_{\max} = \frac{(N-1)xC_{\text{BP}}}{R-(N-1)x} + \frac{(N-1)x^2C_{\text{BP}}}{(R-x)(R-(N-1)x)} \\
&\Rightarrow (N-1)d_{\max}x^2 - (NRd_{\max} + (N-1)C_{\text{BP}}R)x + R^2d_{\max} = 0 \\
&\Rightarrow x = \frac{NRd_{\max} + (N-1)C_{\text{BP}}R \pm \sqrt{(N^2-4N+4)R^2d_{\max}^2 + (N-1)^2C_{\text{BP}}^2R^2 + 2N(N-1)R^2d_{\max}C_{\text{BP}}}}{2(N-1)d_{\max}}, \\
&\text{where} \quad x = L_{\max}/C_{\text{BP}}
\end{aligned} \tag{15}
$$

$$
L_{\max} = \min\left\{ \frac{Nd_{\max}RC_{\text{BP}} + (N-1)C_{\text{BP}}^2R - \sqrt{((N-2)d_{\max}RC_{\text{BP}} + (N-1)RC_{\text{BP}}^2)^2 + 4(N-1)d_{\max}R^2C_{\text{BP}}^3}}{2(N-1)d_{\max}}, \frac{RC_{\text{BP}}}{N} \right\}. \tag{16}
$$

Result 2 can be used to calculate the maximum number of physical block (PB) for one physical protocol data unit (PPDU). Recall from Section III that the L_s is the equivalent protocol overhead and the short MPDU (preamble and frame control), the maximum number of PBs that can be supported by the in-vehicle HPGP is

$$
N_{\text{PB}} = \left\lfloor \frac{L_{\max} - L_s}{136 \cdot 8} \right\rfloor. \tag{17}
$$

where the PB136 (136 bytes per physical block) is considered for Mini-ROBO mode. In priority based multi-access transmission, delay and transmission rate are two important criteria to evaluate the effectiveness of transmission scheduling. Hence, in the following, we explore the inter-relations between these two and propose a rate-adaptive scheduling scheme.

Lemma 1: For each non-highest priority flow, the transmission rate ρ_i is proportional to its maximum access delay $d_i^{\max}$, and has

$$
R - \rho_i \propto \frac{1}{d_i^{\max}}.
$$

Proof: According to (9), we can derive the transmission rate as

$$
\rho_i = R - \frac{L_i \cdot \rho_i^h}{(d_i^{\max} - T_1^*) \cdot (R - \rho_i^h) - \sum_{j=1}^{i-1} L_j}. \tag{18}
$$

where $T_1^* = T_1$ when $i \neq N$, otherwise $T_1^* = 0$. $\rho_i^h = \sum_{j=1}^{i-1} \rho_j$. □

Lemma 1 tells that there is a tradeoff between the transmission rate of priority flow i and its delay performance. According to the definition of transmission rate ρ in (4), a large transmission rate indicates a higher frequency of transmission, which means that contentions with other priority traffic will be increased.

Lemma 2: For each non-highest priority flow, the way to increase the transmission rate without negatively affecting its worst delay performance is to reduce transmission rate of any flow with higher priority.

Proof: According to (18), ρ_i^h is the summation of higher priority transmission rates. Hence, it is straightforward to observe that with a smaller value of ρ_i^h, ρ_i can be increased. □

For the highest priority flow, since $d_1 \leq \frac{max\{L_i|i\in 2...N\}}{R}$, its transmission rate ρ_1 has no effect on its own delay performance, but will impact the performance of lower priority flows. Therefore, combing Lemma 1 and 2, we conclude that a conservative rate scheduling for high priority flow is favorable for low priority flow. Hence we propose the following priority-weighted fair rate scheduling algorithm to maximize the bandwidth utility and maintain delay deadline by imposing the fairness feature into consideration.

Algorithm 1: Priority-Weighted Fair Rate Scheduling

Input: delay requirement $\mathbf{D} = \{d_i | 0 \leq i \leq N\}$, channel capacity R, beacon period C_{BP}, transmission frequency $f = \{f(i) | 0 \leq i \leq N\}$.
Output: rate scheduling $\rho = \{\rho_i | 0 \leq i \leq N\}$.
Initialization: 1) Identify the number of con-current transmission N; 2) Rank their delay requirements with $d_i \leq d_j$, when $i < j$; 3) Calculate the priority weight $w_i = \frac{d_i}{\sum_{i=1}^{N} d_i}$.
for *(each priority flow i to N)* **do**
  $\rho_i = R \cdot w_i$, $L_i = \rho_i \cdot C_{\text{BP}} \cdot f(i)$;
  if $L_i > L_{max}$ *in* (16) **then**
    $L_i = L_{\max}$ // cope with scheduling dynamics;
  if $\rho_i > \rho_i(L_i, d_i)$ *in* (18) **then**
    $\rho_i = \rho_i(L_i, d_i)$ // without violating max. delay;
  Configure $N_{\text{PB}}(i)$ in (17) to accommodate physical blocks packaging.

VI. Queuing Delay Analysis on Switch Port

So far, the worst delay of medium access over a single bus has been shown a bounded performance by using the NC. The calculation of transmission delay is straightforward by having $d_{trans} = L_i/R$. However, message exchange between bus systems are usually needed in vehicle system, and thus

the delay issue has been shifted from channel contention to congestion on switch port.

The IEEE 802.1 Audio Video Bridging (AVB) [38] is being actively considered as a promising solution to automotive time-sensitive applications. One of the key mechanisms to ensure E2E delay performance is to use the traffic shaper to regulate priority flows on switch port. Therefore, in this section, we characterize the queuing delay on switch and further propose an effective shaping solution to guarantee the E2E delay performance using HPGP.

A. Traffic shaper in IEEE 802.1 AVB

The traffic shaping algorithm in IEEE 802.1 AVB defines two stream reservation (SR) classes which are with higher priority than the traditional strict priority (SP)[4] traffic class. Each SR class defines both idle-slope R_{IS} which is the rate of gaining credit, and send-slope R_{SS} which is the rate of reducing the credit, and has

$$R_{SS} = R_{IS} - R\,, \tag{19}$$

where R is the capacity of the channel. However, different to the standard approach which is originally used for multimedia services in Ethernet, the number of SR class for the mission-critical vehicle application is determined by the number of in-vehicle messages requiring guaranteed E2E delay. Thus, we assume the number of SR class is identical to N.

Result 3: The ratio $\eta = \left|\frac{R_{IS}}{R_{SS}}\right|$ defines forwarding efficiency of SR class and has

$$\eta = \begin{cases} \leq 1, & \text{Less burst data transmitted than SP.} \\ > 1, & \text{More burst data transmitted than SP.} \end{cases}$$

Proof: We denote t_{acc} as the time duration of accumulating credit and R_{IS} as the service rate of a SR class. According to the credit-based traffic shaper policy defined by the AVB, the total amount of data accumulated and forwarded by a SR class can be expressed as

$$\begin{aligned} \rho_{acc} &= R_{IS} \cdot t_{acc}\,, \\ \rho_{fwd} &= R_{IS} \cdot t_{acc} \cdot \eta\,. \end{aligned} \tag{20}$$

When $\eta \leq 1$, $\rho_{fwd} \leq \rho_{acc}$, the total accumulated queuing data may not be fully forwarded by switch and the queue is expected to increase. The amount of burst data pushed onto the channel is no larger than SP.

When $\eta > 1$, $\rho_{fwd} > \rho_{acc}$, the switch allows more queuing data to be forwarded, particularly when the SR is with stringent delay deadline but more congested data on the queue. The SR will generate more burst data over the channel. □

The result shows that the principle of the traffic shaper is to limit the amount of burst data pushed onto the channel, which affects the delay performance of other priority flows. In the following, we propose a delay sensitive shaping algorithm to dynamically adjust the forwarding speed of each queue according to its priority and residual delay time.

[4]The strict priority (SP) class has been used to characterize access delay.

B. Delay Sensitive Traffic Shaper

Our objective is to find a strategy that determines η for each incoming flow and ensures its E2E delay performance. It is worth noting that both idle-slope and send-slope of a flow also affect the performance of other flows. When multiple queues are competing on a switch port, we expect the overall delay requirements can be satisfied.

To reflect the residual time budget of a priority flow and adjust the corresponding service rate to satisfy its delay requirement when it arrives at switch, we define the forwarding efficiency of flow i as

$$\eta_i = \frac{T_{consumed}}{T_{residual}} = \frac{T_{consumed}}{T_{target} - T_{consumed}}\,, \tag{21}$$

The rational behind (21) is to satisfy a global delay requirement by reshaping the service curves, particularly for those flows with lower priority and residual delay budget.

By keeping the same service rate R_i as defined in Section IV-B for each priority flow, we define the idle-slope R_{IS} for priority i as

$$R^i_{IS} = R_i\,, \tag{22}$$

Hence the corresponding send-slope R_{SS} can be defined as

$$R^i_{SS} = \frac{R^i_{IS}}{\eta}\,. \tag{23}$$

The delay analysis has now been shifted from a contention problem over a single bus to a congestion problem on switch port. We can still apply the approach in Section IV-B to obtain the rate-latency service curve for each priority flow.

1) Highest priority: The highest priority traffic can always be scheduled for forwarding, unless there is a lower priority frame in transmission. Thus the rate-latency curve is

$$\beta^1(t) = R^1 \cdot (t - T^1)^+\,. \tag{24}$$

where $R^1 = R$ and $T^1 = \frac{max\{L_i | i \in 2...N\}}{R}$ which is the maximum transmission delay of a low priority data.

2) Lower priority: For any lower priority flow i using SR class, its delay T^i is highly related to the delay time from all higher SR priority flows. The time period of send-slope R^i_{SS} can be expressed as

$$t^i_{SS} = \frac{T^i R^i + offset^i}{R^i_{SS}}\,, \tag{25}$$

where $R^i = R_i$, $R^i_{SS} = \frac{R^i}{\eta}$ and $offset^i = R^i_{SS}\frac{L_i}{R}$ is the one maximum frame that can be transmitted when the credit of i is closed to 0, which brings the total credit goes to negative. Thus, we can obtain the delay

$$T^i = T^1 + \sum_{j=1}^{i-1} t^j_{SS} = T^1 + \sum_{j=1}^{i-1} \frac{T^j R^j + offset^j}{R^j_{SS}}\,, \tag{26}$$

Therefore, the service curve is derived as

$$\beta^i(t) = R^i \cdot (t - T^i)^+\,. \tag{27}$$

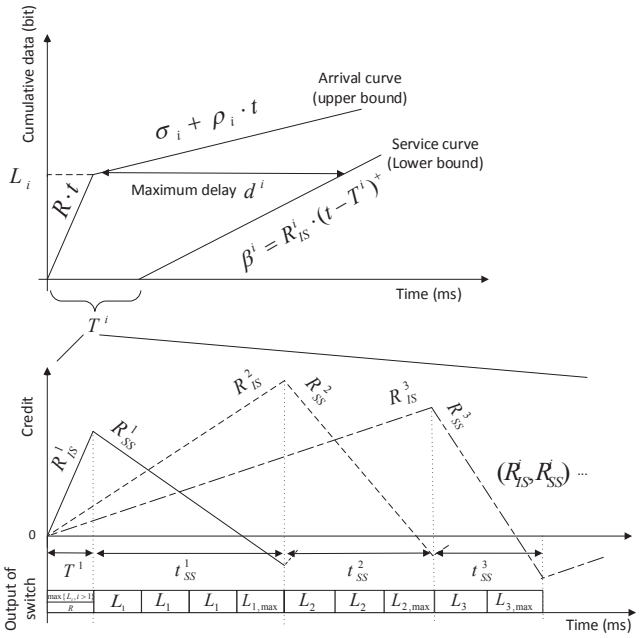

Fig. 3. Queuing delay of SR based transmission on switch

3) Maximum queuing delay: The derived Theorem 1 can still be applied to derive the bounded queuing delay for each priority i, thus the queuing delay bound is

$$d^i \leq T^i + \frac{\sigma_i \cdot (R - R^i)}{(R - \rho_i) \cdot R^i} . \tag{28}$$

Fig. 3 illustrates the SR based transmission on switch port. It is noted that the SP based traffic class can coexist with SR class, and serve priority flows which miss the delay deadline. In such a case, a best-effort approach will be adopted.

C. End-to-end Delay

Combine the access, transmission and queuing delay that we have analyzed so far, the worst E2E delay of priority i can be derived as

$$D^i_{E2E} \leq d_i + \frac{L_i}{R} + d^i , \tag{29}$$

The result can be further generalized to a more complex network scenarios with multiple bus systems crossing the same switch or cascaded networks. Thus the worst E2E delay can be derived as

$$\hat{D}^i_{E2E} \leq \sum_{h=1}^{n} (d_{i|h} + \frac{L_i}{R} + d^{i|h} \left(\eta_i = \max\{\eta_i^k\}, k = 1...m\right)) . \tag{30}$$

where n is the number of hops, each hop is composed of a communication bus and a switch. m is the number of bus systems crossing one switch. The flows with the same priority are scheduled on the same queue when they arrive at the same switch port. By choosing a maximum η_i among different systems, the lower bound service curve can be guaranteed for all priority flow i crossing the same switch.

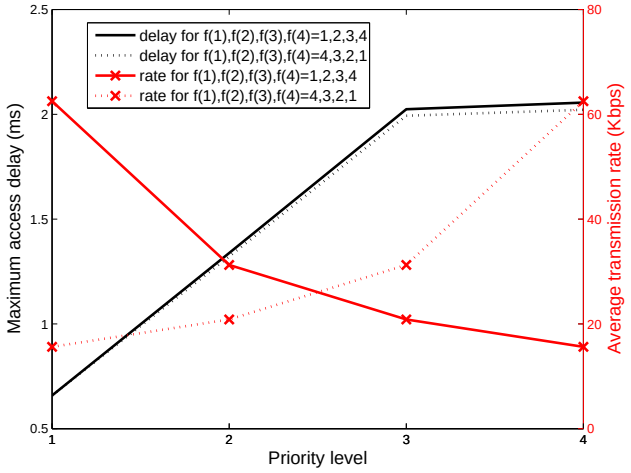

Fig. 4. Maximum delay and transmission rate for original HPGP

VII. Performance Evaluation

In this section, we provide evaluation results using the system parameters provided in Section III.

A. Original HPGP

Fig. 4 shows the maximum delay and transmission rate for each priority flow, respectively, with two sets of cycle rates and identical frame length, i.e., $L_i = L_s, i \in 1...N$. The general delay performance of all flows aligns with Result 1. We can also observe that the delay performance is negatively affected by the decreasing priority. Moreover, if higher priority flows tend to increase their cycle rate (or reduce their transmission rate), the delay of lower priority flows will be improved, which is relevant to Lemma 2.

We also compare the maximum delay bounds (incremented by transmission delay) among four major solutions obtained using NC in Fig. 5(a). In the comparison, both LIN and CAN based solutions are using the identical data size of 8 byte and 4 priorities. The basic cycle length are the same as $C_{\text{BP}} = 40$ ms, each priority flow can be sent at a rate of $f(i) \cdot C_{\text{BP}}$, where $f(i)$ is an integer value chosen by flow i. According to the standard specification, the LIN bus [3] uses the master-slave periodical transmission with date rate of 20 Kbps, whereas the CAN [2] bus uses priority-based contention detection and resolution (CDR) with date rate of 250 Kbps. The latest Multi-channel CAN (M-CAN) [9] is based on the high-speed CAN (500 Kbps) but with two frequency selection. Their delay bounds are derived in Appendix A. The simulation is also supplemented by having 4 collision-free nodes over a single bus with different priority, randomly selected cycle frequency and destinations. The result is collected as the worst delay over 100 beacon periods. It can be seen that the HPGP shows clear advantage over the LIN, but with competitive performance against CAN based protocols. Since HPGP introduces extra overhead compared with other solutions, Fig. 5(b) shows a fair comparison by averaging the delay performance, i.e., delay

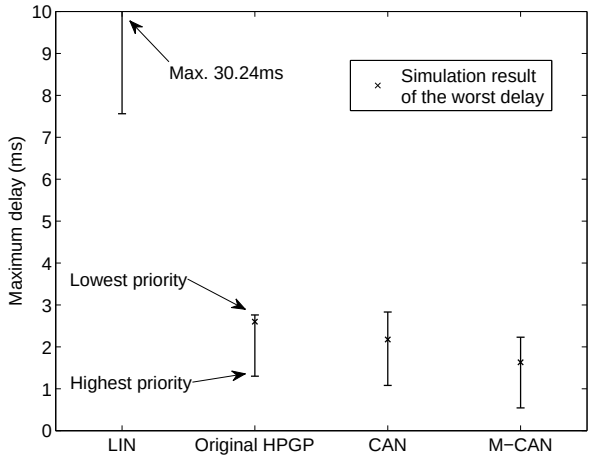

(a) Delay performance for transmitting one 8-Byte control data: LIN (108 bits), Original HPGP (2500 bits), CAN and M-CAN (136 bits)

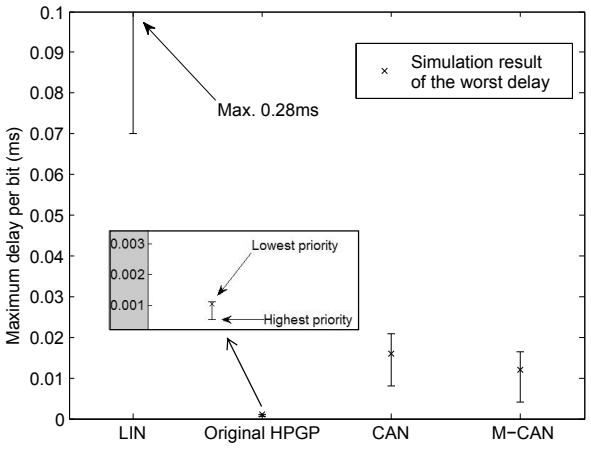

(b) Average delay performance for transmitting one 8-Byte control data

Fig. 5. Maximum delay comparisons for 4 priorities

time per bit. The HPGP shows the superior performance than CAN based protocols.

Table V shows the result of the scheduled transmission rate and achievable delay performance by applying Algorithm 1 for original HPGP and CAN, respectively. In this example, we simply configure $F_1 = F_2 = F_3 = F_4 = C_{\text{BP}}$. As can be seen, the derived result can keep the actual delay performance within the targeted delay deadline. Moreover, by adjusting the payload size, adaptive transmission rates can be achieved to support more data type, e.g., multimedia, in order to maximize the bandwidth utility. The fairness index (ρ/d_{target}) indicates that the proposed solution can successfully maintain a global fairness by allocating more bandwidth to low priority flows. Moreover, we should note that given the same priority and delay requirements, HPGH can support much higher transmission rate and more payload than the CAN solution.

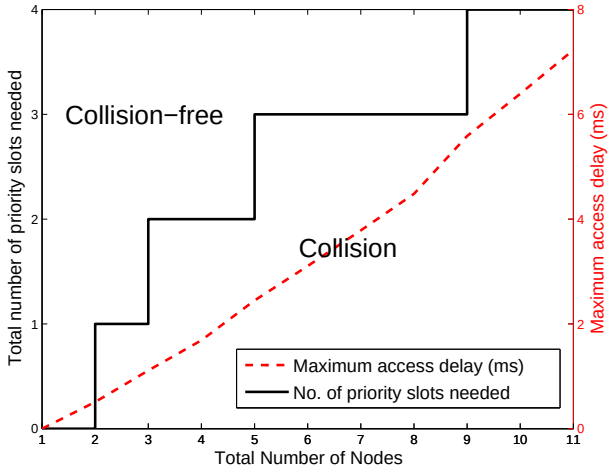

Fig. 6. No. of priority slots needed and its maximum access delay under different network size

B. Collision-Free HPGP

Fig. 6 shows the relations between the number of nodes on a single bus, priority time slots needed and their maximum access delay performance. All nodes are transmitting using the identical frame length, i.e., $L_i = L_s, i \in 1...N$. The result can be used to determine the maximum number of collision-free nodes and its priority slots configuration when delay requirement is known.

We further compare the maximum delay bounds (incremented by transmission delay) among the same solutions in Fig. 7(a). The benchmark solutions are using the same data model and cycle rate assumed in Fig. 5(a). According to Table IV, the collision-free HPGP for $N = 10$ uses $L_s = 2296$ bits. We notice that the worst delay of the lowest priority flow using the proposed collision-free HPGP is worse than that of CAN bus, whereas in Fig. 5(a), such delay is better than CAN. The result indicates that due to the large overhead and exchange complexity of HPGP, its performance tends to worse than CAN when the number of node increases over a single bus. However, the average delay performance of collision-free HPGP in Fig. 7(b) is still the best among all solutions.

By further applying the Algorithm 1 into the collision-free HPGP and CAN to cope with more ECUs sharing on the same bus, Table VI shows the optimized transmission rate and delay performance. It is clear that the proposed fair scheduling works well for both collision-free HPGP and CAN. It is also interesting to observe that for priority 1 and 2, the maximum payload of HPGP is 16 bytes, which means that only control frame is used for data transmission. The result is also aligned with the general practise that time-critical control messages are usually assigned with higher priority but small data size, whereas for less-critical data transmission, high data rate and large packet size is allowed but with lower priority. The data rate and maximum payload spreads even wider when more priority flows are transmitting, HPGH still achieves a better performance than the CAN solution.

TABLE V
PRIORITY-WEIGHTED FAIR RATE SCHEDULING FOR ORIGINAL HPGP AND CAN

	Original HPGP				CAN			
Priority level	1	2	3	4	1	2	3	4
Targeted access delay (ms)	10	20	30	40	10	20	30	40
Achieved delay (ms)	6.1	9.2	17.8	40	6.04	9.1	17.8	40
Transmission rate (Mbps)	0.24	0.76	1.14	1.44	0.015	0.05	0.075	0.094
Maximum payload (Byte)	832	1648	2192	2600	64	112	152	176
Bandwidth utility	94.2% (3.58 Mbps/3.8 Mbps)				93.6% (234 Kbps/250 KBps)			
Jain's fairness	97.16%				97.15%			

TABLE VI
PRIORITY-WEIGHTED FAIR RATE SCHEDULING FOR COLLISION-FREE HPGP AND CAN

	Collision-Free HPGP							CAN						
Priority level	1	2	3	4	5	6	7	1	2	3	4	5	6	7
Targeted access delay (ms)	4	5	10	15	20	30	40	4	5	10	15	20	30	40
Achieved delay (ms)	3.2	3.8	4.7	6.5	10	17	36.4	3.1	3.8	4.6	6.5	9	17	36.4
Transmission rate (Mbps)	0.05	0.15	0.31	0.46	0.61	0.92	1.22	0.003	0.01	0.02	0.03	0.04	0.06	0.08
Maximum payload (Byte)	16	16	288	560	696	968	1241	8	8	24	40	56	72	88
Bandwidth utility	97.8% (3.72 Mbps/3.8 Mbps)							97.2% (243 Kbps/250 Kbps)						
Jain's fairness	96.03%							96%						

C. End-to-end Delay Analysis

In this section, we further incorporate queuing delay into analysis. We assume that a bus system is composed of 7 priority nodes, and bus systems are connected by switches. All nodes in a bus are transmitting using the identical frame length, i.e., $L_i = 2160\,\text{bits}, i \in 1...N$, according to Table IV. In order to derive the worst delay, the transmission frequency is assumed to be the same for all priority flows, that is, $F_i = C_{\text{BP}}, i \in 1...N$.

In order to compare and analyze the access and queuing delay, we start with a simple scenario where only one bus system is directly connected with one switch, e.g., Fig. 1 (b). Fig. 8 shows the breakdown of E2E delay when a frame is transmitted over the bus, arrived and forwarded by the switch. It shows that the priority 2 and 3 using the proposed time sensitive shaper on switch have a lower delay than SP over the bus, whereas for the priority 4-7, such delay is worse than SP. This is because after the SP transmission over the bus, the priority flows 2 and 3 have lower residual delay budget compared with other priorities. Hence, according to the proposed delay sensitive shaper, it will allocate more transmitting time (with a relatively small send-slop) when priority 2 and 3 are engaged for forwarding. Such adaptive changes will increase the delay of lower priority flows, however, the proposed time sensitive shaper can still maintain their worst delay performance within the deadline. Furthermore, because the dynamic adjustment of traffic considers both consumed and residual delay budgets, the proposed solution can maintain a global fairness among all priority flows in order to avoid missing the deadline of any priority flow. The Jain's fairness index ($d_{achieved}/d_{target}$) in Fig. 8 can reach to 92.46%.

Fig. 9 further compares the E2E delay performance by using different shaper solutions on switch port, such as SP, IEEE 802.11 AVB [38][5] and weighted round robin [30]. It shows that under the same network assumption and delay deadline, the proposed solution is the only one that can manage to keep the E2E delay within the target delay deadline. Table VII also shows the statistics of delay performance. The value with "*" indicates the violation of delay deadline.

TABLE VII
STATISTICS OF ACHIEVED END-TO-END DELAY PERFORMANCE

Priority level	1	2	3	4	5	6	7
Targeted E2E delay (ms)	5	5	4	6	10	15	20
Proposed delay sensitive shaper (ms)	1.7	2.5	3.5	5.6	8.9	12.5	15.8
SP (ms)	1.7	1.9	**4.1***	5.3	6.6	7.9	8.1
AVB (ms)	1.7	2.5	**4.6***	**6.5***	8.4	10.3	11.2
RR (ms)	**8***	**8.6***	**9.2***	**9.8***	**10.5***	11.11	11.12

In order to show the delay performance in a more complex in-vehicle network scenario, we consider a network topology in Fig. 10 in which the bus network A is transmitting to D, B is transmitting to A, and C is transmitting to D, simultaneously. Transmitting nodes in both B and C are with the same delay deadlines, whereas A is with more relaxed deadline due to the multi-hop transmission. The result in Fig. 11 shows that the actual delay of all flows can be maintained within the deadline by using the proposed shaper method. It is also interesting to observe that the system C performs worse than B although they have the same delay constraints. This is because the network C is competing with A on switch 2 when A has relatively lower residual budget compared itself on switch 1, thus the proposed delay sensitive shaper allocates more transmission time for A on switch 2, which leads to a worse delay performance for C. However, B has the advantage to compete with A on switch 1 when both A and B have adequate delay budget.

[5]In the standard AVB, only two SR classes are considered and lower priority flows are using SP.

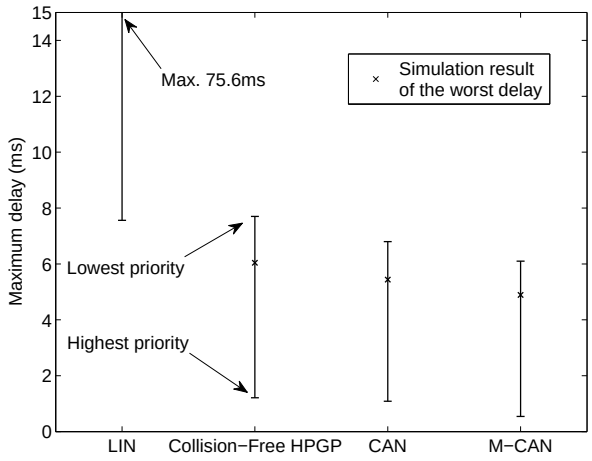

(a) Delay performance for transmitting one 8-Byte control data: LIN (108 bits), Collision Free HPGP (2296 bits), CAN and M-CAN (136 bits)

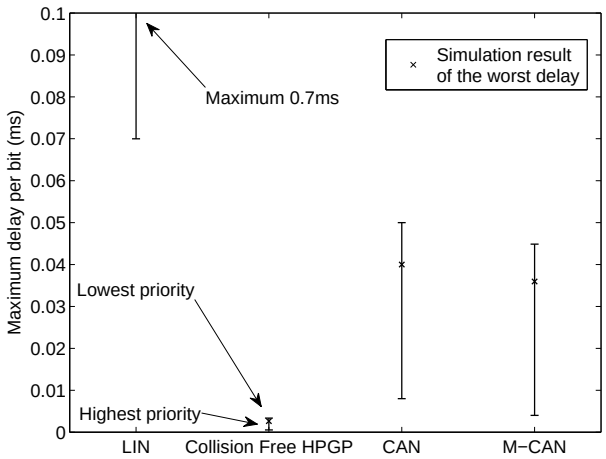

(b) Average delay performance for transmitting one 8-Byte control data

Fig. 7. Maximum delay comparisons for 10 priorities

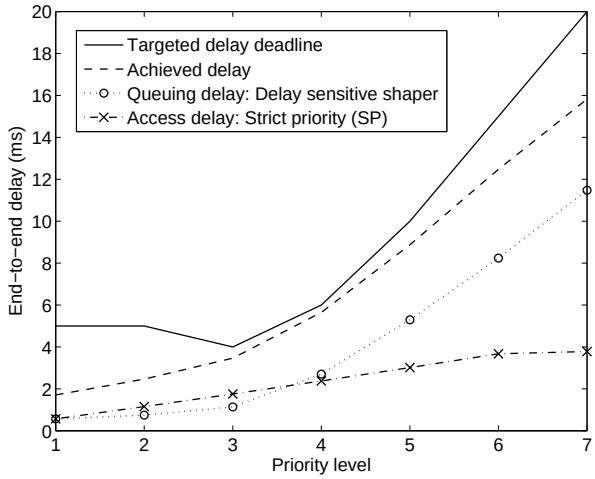

Fig. 8. Breakdown of end-to-end delay in a single bus and switch scenario

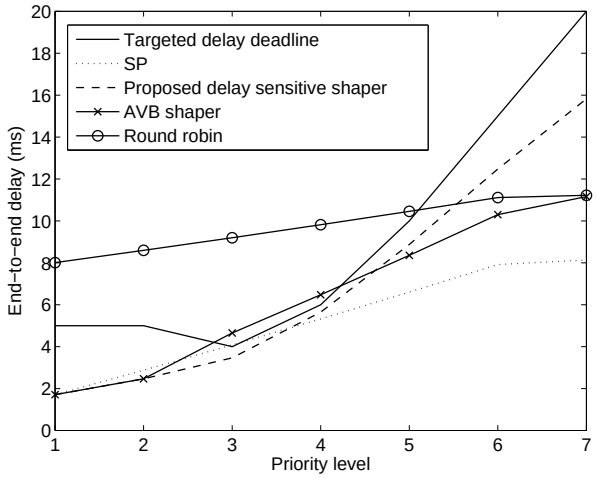

Fig. 9. Comparison of end-to-end delay using different traffic shaper

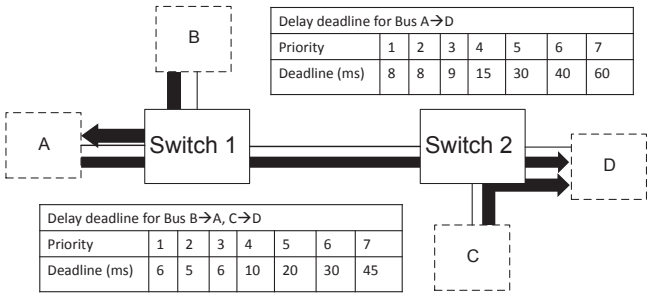

Fig. 10. A multi-hop and cross-domain scenario with traffic delay constraints

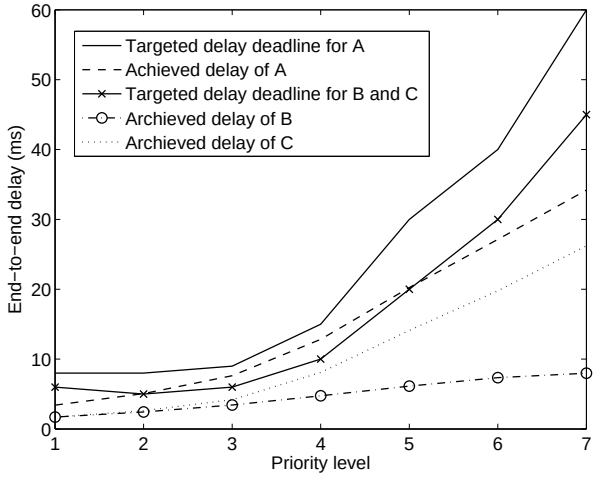

Fig. 11. End-to-end delay comparison in a multi-hop and cross-domain scenario using the proposed delay sensitive shaper

VIII. Conclusions

We have shown that HPGP is able to meet hard delay requirement of in-vehicle communications. Even in the condition of high workload, the performance of the integrated design of contention and congestion control is adequate and promising for in-vehicle power line networks. Compared with the industry solutions, the HPGP based approach is promising to replace the legacy LIN and low/medium speed CAN. The results can be used to help vehicle and networking engineers design HPGP-based mission critical applications and future network infrastructure in vehicular environments to integrate every "object" (e.g., in-vehicles' sensors, passengers' smart phones, infrastructures) and form an intelligent transportation system. The in-vehicle communications discussed in this paper can be used to connect in-vehicle components with the external world, which will increase the support of human and machine communications in connected vehicles.

Appendix A
Delay calculation for existing solutions

A. LIN

It is a single master/multiple slave architecture. One node, termed the master, possesses an accurate clock and drives the communication by polling the other nodes, the slaves, periodically. A master can handle at most 15 slaves (there are 16 identifiers by class of data length). As it is time triggered, message latency is guaranteed. The transmission rate is 20 Kbps and the data length is 8 bytes.

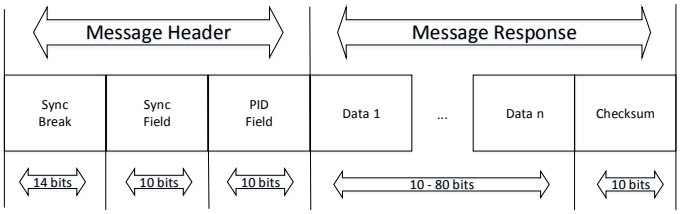

Fig. 12. Time schedule of LIN bus transmission [3]

Fig. 12 shows the time schedule for transmitting a LIN message. The message header takes 34 bits (14 bits+10 bits+10 bits) and the response takes 74 bits (8×8 bits+10 bits). The total number of bit is 108 bits (34 bits+74 bits). Therefore, the transmission delay is:

$$D_t = \frac{108}{20\,\text{Kbps}} = 5.4\,\text{ms}\,, \tag{31}$$

A time reserve of up to 40% is given for transmission of a LIN message, that is, interbyte space. Hence the delay for transmitting one message is

$$D_t^* = D_t * 1.4 = 7.56\,\text{ms}\,. \tag{32}$$

Therefore, the maximum delay for the first scheduled node (or with the highest priority) is $D_{LIN}^h = 7.56\,\text{ms}$, whereas the maximum delay for the last node (or with the lowest priority N) is $D_{LIN}^l = N \times 7.56\,\text{ms}$.

B. CAN

CAN is a priority-based bus which allows to provide a bounded communication delay for each message priority. The MAC protocol of CAN uses CSMA/CDR with bit by bit non-destructive arbitration over the ID field (Identifier). In our case, we consider that the identifier is coded using 11 bits (CAN 2.0A) and it also serves as priority. Higher priority messages always gain access to the medium during arbitration. The data size is also considered as 8 bytes and transmission rate is 250 Kbps.

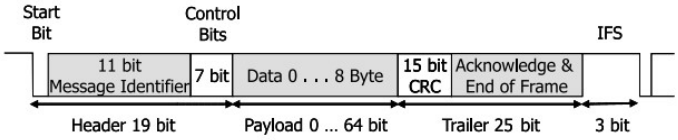

Fig. 13. CAN frame structure [2]

Fig. 13 shows the CAN frame structure, the equivalent maximum frame size of CAN is 136 bits (130 bits maximum frame size plus 6 bits carrier sensing time). Since CAN is also a priority based protocol, we can use the similar result from Theorem 1 and obtain the delay performance as follows. The data length is $L = 136$ bits, the cycle rate for all priority flows is set at its maximum $F_i = 40\,\text{ms}$, and $R = 250\,\text{Kbps}$. Therefore, the maximum delay for the highest priority node is

$$D_{CAN}^h = \frac{2L}{R} = \frac{2 \times 136}{250\,\text{Kbps}} = 1.088\,\text{ms}\,. \tag{33}$$

The maximum delay for the lowest priority node depends on the number of priorities N, and can be derived as

$$D_{CAN}^l = \frac{(N+1)L}{R - \rho_i^h} = \frac{(N+1) \times 136}{250\,\text{Kbps} - (N-1) \times 136/40\,\text{ms}}\,. \tag{34}$$

It is worth noting that CAN bus has 11 priority bits, which means that it can theoretically cope with 2048 priority levels.

C. Multi-channel CAN [9]

The result of Multi-channel CAN (M-CAN) can be derived directly from the standard CAN bus. We consider the high-speed CAN with a total transmission rate of 500 Kbps. Since the M-CAN employs two frequency channels characterized by power lines, the maximum delay results can be obtained as

$$D_{M-CAN}^h = \frac{L}{R} = \frac{136}{250\,\text{Kbps}} = 0.544\,\text{ms}\,. \tag{35}$$

It is noted that the effective data rate for each channel is $R = 250\,\text{Kbps}$ and the highest priority flow (with the minimum delay) can have the privilege to dominate a single channel.

The maximum delay for the lowest priority node depends on the number of priorities N, and can be derived as

$$D_{CAN}^l = \frac{NL}{R - \rho_i^h} = \frac{N \times 136}{250\,\text{Kbps} - (N-2) \times 136/40\,\text{ms}}\,. \tag{36}$$

Since there are always two channels available, the worst delay happens when up to $N-1$ nodes sharing a single channel.

REFERENCES

[1] W. Fleming, "Forty-year review of automotive electronics: A unique source of historical information on automotive electronics," *IEEE Veh. Tech. Mag.*, vol. 10, no. 3, pp. 80–90, Sept 2015.

[2] "CAN specification version 2.0," in *Robert Bosch GmbH*, 1991.

[3] "LIN specification package revision 2.1," in *LIN Consortium*, 2006.

[4] M. Johas Teener, A. Fredette, C. Boiger, P. Klein, C. Gunther, D. Olsen, and K. Stanton, "Heterogeneous networks for audio and video: Using ieee 802.1 audio video bridging," *Proc. of the IEEE*, vol. 101, 2013.

[5] L. Bello, "Novel trends in automotive networks: A perspective on ethernet and the ieee audio video bridging," in *Proc. IEEE Emerging Technology and Factory Automation (ETFA)*, Sept 2014, pp. 1–8.

[6] S. Kehrer, O. Kleineberg, and D. Heffernan, "A comparison of fault-tolerance concepts for ieee 802.1 time sensitive networks (tsn)," in *Proc. IEEE Emerging Technology and Factory Automation (ETFA)*, Sept 2014.

[7] "Using power line communication to reduce harness in automotive," in *Yamar*, http://yamar.com/articles/Using-power-line-communication-to-reduce-harness-in-automotive.pdf.

[8] M. Strobl, T. Waas, S. Moehne, M. Kucera, A. Rath, N. Balbierer, and A. Schingale, "Using ethernet over powerline communication in automotive networks," in *Proc. WISES*, 2012, pp. 39–44.

[9] Z. Sheng, A. Kenarsarii, N. Taherinejad, and V. Leung, "A multichannel medium access control protocol for vehicular power line communication systems," *IEEE Trans. on Veh. Tech.*, vol. 65, no. 2, 2016.

[10] J.-Y. Le Boudec and P. Thiran, *Network Calculus: A Theory of Deterministic Queuing Systems for the Internet*. Springer-Verlag, 2001.

[11] M. Fidler, "Survey of deterministic and stochastic service curve models in the network calculus," *IEEE Commu. Surv. Tut.*, vol. 12, 2010.

[12] J. Huang, Y. Sun, Z. Xiong, Q. Duan, Y. Zhao, X. Cao, and W. Wang, "Modeling and analysis on access control for device-to-device communications in cellular network: A network-calculus-based approach," *IEEE Trans. Veh. Tech.*, vol. 65, no. 3, pp. 1615–1626, March 2016.

[13] Z. Tao, W. Quan, and W. Gao-Cai, "Performance analysis on m2m communication network based on stochastic network calculus," in *Proc. IEEE Int. Conf. on Trust, Security and Privacy in Computing and Communications*, 2014, pp. 865–870.

[14] J. Xie and Y. Jiang, "A network calculus approach to delay evaluation of ieee 802.11 dcf," in *Proc. IEEE Conf. on Local Computer Networks (LCN)*, 2010, pp. 560–567.

[15] K. Katsaros, M. Dianati, R. Tafazolli, and G. Xiaolong, "End-to-end delay bound analysis for location-based routing in hybrid vehicular networks," *IEEE Trans. Veh. Technol.*, vol. PP, no. 99, pp. 1–1, 2015.

[16] A. Albert, "Comparison of event-triggered and time-triggered concepts with regards to distributed control systems," in *Proc. Embedded World Conf.*, 2004, pp. 235–252.

[17] N. Taherinejad, R. Rosales, S. Mirabbasi, and L. Lampe, "A study on access impedance for vehicular power line communications," in *Proc. IEEE Int. Symp. on Power Line Communications and Its Applications (ISPLC)*, Udine, Italy, Apr. 2011, pp. 440 –445.

[18] A. Pittolo, M. D. Piante, F. Versolatto, and A. M. Tonello, "In-vehicle power line communication: Differences and similarities among the in-car and the in-ship scenarios," *IEEE Veh. Technol. Mag.*, vol. 11, no. 2, pp. 43–51, 2016.

[19] N. Taherinejad, R. Rosales, L. Lampe, and S. Mirabbasi, "Channel characterization for power line communication in a hybrid electric vehicle," in *Proc. IEEE Int. Symp. on Power Line Communications and Its Applications (ISPLC)*, March 2012, pp. 328–333.

[20] M. Lienard, M. O. Carrion, V. Degardin, and P. Degauque, "Modeling and analysis of in-vehicle power line communication channels," *IEEE Trans. Veh. Technol.*, vol. 57, no. 2, pp. 670–679, 2008.

[21] P. Degauque, I. Stievano, S. Pignari, V. Degardin, F. Canavero, F. Grassi, and F. J. Canete, "Power-line communication: Channel characterization and modeling for transportation systems," *IEEE Veh. Technol. Mag.*, vol. 10, no. 2, pp. 28–37, 2015.

[22] D. Hristu-Varsakelis and W. Levine, *Handbook of Networked and Embedded Control Systems*. Birkhuser Basel, 2005.

[23] A. Chandra, A. Proke, T. Mikulek, J. Blumenstein, P. Kukolev, T. Zemen, and C. F. Mecklenbruker, "Frequency-domain in-vehicle uwb channel modeling," *IEEE Trans. Veh. Technol.*, vol. 65, no. 6, pp. 3929–3940, 2016.

[24] S. Tuohy, M. Glavin, C. Hughes, E. Jones, M. Trivedi, and L. Kilmartin, "Intra-vehicle networks: A review," *IEEE Trans. Intel. Trans. Sys.*, 2015.

[25] S. Woo, H. J. Jo, and D. H. Lee, "A practical wireless attack on the connected car and security protocol for in-vehicle can," *IEEE Trans. Intell. Transp. Syst.*, vol. 16, no. 2, pp. 993–1006, 2015.

[26] T. Gehrsitz, H. Kellermann, H.-T. Lim, and W. Kellerer, "Analysis of medium access protocols for power line communication realizing in-car networks," in *Proc. IEEE Veh. Tech. Conf. (VTC Fall)*, Sept 2014, pp. 1–7.

[27] T. Gehrsitz, R. Durner, H. Kellermann, H.-T. Lim, and W. Kellerer, "Priority-based energy-efficient mac protocols for the in-car power line communication," in *Proc. IEEE Veh. Netw. Conf. (VNC)*, Dec 2014, pp. 61–68.

[28] R. Antonioli, M. Roff, Z. Sheng, J. Liu, and V. Leung, "A real-time mac protocol for in-vehicle power line communications based on homeplug gp," in *Proc. IEEE Veh. Tech. Conf. (VTC Spring)*, 2015, pp. 1–5.

[29] J.-P. Georges, T. Divoux, and E. Rondeau, "Strict priority versus weighted fair queueing in switched ethernet networks for time critical applications," in *Proc. IEEE Intl. Paral. and Dist. Proc. Symp.*, 2005, pp. 141–141.

[30] M. Manderscheid and F. Langer, "Network calculus for the validation of automotive ethernet in-vehicle network configurations," in *Proc. Int. Conf. on Cyber-Enabled Distributed Computing and Knowledge Discovery (CyberC)*, 2011, pp. 206–211.

[31] R. Queck, "Analysis of ethernet avb for automotive networks using network calculus," in *Proc. IEEE Int. Conf. Vehicular Electronics and Safety (ICVES)*, 2012, pp. 61–67.

[32] M. Rahmani, K. Tappayuthpijarn, B. Krebs, E. Steinbach, and R. Bogenberger, "Traffic shaping for resource-efficient in-vehicle communication," *IEEE Trans. Ind. Informat.*, vol. 5, no. 4, pp. 414–428, 2009.

[33] G. Xie, G. Zeng, R. Kurachi, H. Takada, and R. Li, "Gateway modeling and response time analysis on can clusters of automobiles," in *Proc. IEEE Int. Conf. on Embedded Software and Systems (ICESS),*, 2015, pp. 1147–1153.

[34] U. Klehmet, T. Herpel, K. Hielscher, and R. German, "Delay bounds for CAN communication in automotive applications," in *Proc. MMB*, 2008.

[35] M. Rahmani, R. Steffen, K. Tappayuthpijarn, E. Steinbach, and G. Giordano, "Performance analysis of different network topologies for in-vehicle audio and video communication," in *Proc. Int. Telecommu. Netw. Workshop on QoS in Multiservice IP Networks*, Feb 2008, pp. 179–184.

[36] L. C. Wolf, C. Griwodz, and R. Steinmetz, "Multimedia communication," *Proc. IEEE*, vol. 85, no. 12, pp. 1915–1933, 1997.

[37] "DTA s80pro ECU," in *DTA*, http://www.dtafast.co.uk/dta_products/s80pro-ecu/.

[38] "Virtual bridged local area networks amendment 12: Forwarding and queuing enhancements for time-sensitive streams," in *IEEE Std 802.1Qav-2009*, 2009.